TÜBİTAK

Turk J Elec Eng & Comp Sci, Vol.20, No.2, 2012, © TÜBİTAK
doi:10.3906/elk-1101-1051

Training data optimization for ANNs using genetic algorithms to enhance MPPT efficiency of a stand-alone PV system

Ahmet Afşin KULAKSIZ*, Ramazan AKKAYA
Department of Electrical and Electronics Engineering, Faculty of Engineering and Architecture, Selçuk University,42075 Konya-TURKEY
e-mails: {afsin, akkaya}@selcuk.edu.tr

Received: 25.01.2011

Abstract

Maximum power point tracking (MPPT) algorithms are used to force photovoltaic (PV) modules to operate at their maximum power points for all environmental conditions. In artificial neural network (ANN)-based algorithms, the maximum power points are acquired by designing ANN models for PV modules. However, the parameters of PV modules are not always provided by the manufacturer and cannot be obtained readily by the user. Experimental measurements implemented in the overall PV system may be used to obtain the ANN dataset. One drawback of this method is that the generalization ability of the neural network usually degrades and some data reducing the effectiveness of the network may exist. A genetic algorithm can be used to automatically select the important data among all the inputs, resulting in a smaller and more effective dataset. In our study, a genetic algorithm is used to improve the MPPT efficiency of a PV system with induction motor drive by optimizing the input dataset for an ANN model of PV modules. A variable frequency volts-per-Hertz (V/f) control method is applied for speed control of the induction motor, and a space-vector pulse-width modulation (SV-PWM) method is used to operate a 3-phase inverter. Both simulation and experimental results are presented to demonstrate the validation of the method.

Key Words: *Photovoltaic systems, artificial neural networks, genetic algorithms, space-vector pulse-width modulation*

1. Introduction

Photovoltaic (PV) systems, making use of the renewable source of solar energy, draw increasing attention due to improvements in PV technology, environmental concerns, and their lack of fuel costs. The relatively low conversion efficiency of PV modules encourages the use of maximum power point tracking (MPPT) methods to increase the efficiency of PV systems. PV cells have a nonlinear relationship between the current and

*Corresponding author: Department of Electrical and Electronics Engineering, Faculty of Engineering and Architecture, Selçuk University, 42075 Konya-TURKEY

the voltage, and the maximum power point (MPP) of PV cells changes with environmental conditions such as solar irradiance and ambient temperature. Therefore, MPPs must be estimated using direct or indirect methods, which are used to match the PV source and the load impedance for all environmental conditions to ensure maximum power generation from PV modules. In recent years, numerous MPPT methods have been proposed. Those most commonly used are the lookup-table method [1], perturb and observe (P&O) method [1-3], incremental conductance method [1,4], and artificial intelligence methods [1,5-8]. The drawback of P&O method is that, at steady state, the operation point oscillates around the MPP. The P&O and incremental conductance methods furthermore do not perform well in rapidly changing atmospheric conditions, which make them less favorable [1].

The ability of artificial neural networks (ANN) to construct complex nonlinear mapping through a training process makes them a suitable alternative in the field of PV technology. Using the noise-rejection capability of ANNs, problems such as oscillations around the MPP and trapping in local points can be alleviated [5]. Using an ANN-based method, no prior knowledge of the physical parameters related to the components of the PV system is required. In our research, experimental measurements implemented in the PV system are used to obtain an ANN dataset, which is used to extract a relationship between the input and the output.

Several authors have demonstrated that, by using the genetic algorithm (GA) approach in dataset optimization, a better performance can be obtained compared to approaches using only input datasets [9,10]. In our research, GA optimization is used to enhance the accuracy of an ANN-based MPPT algorithm. The GA is used to automatically select the important data from among all inputs, and a smaller and more effective dataset is obtained. The MPPT algorithm was employed in a stand-alone PV system with a direct-coupled induction motor drive, which employs only an inverter stage to extract maximum power from PV modules. MPPT was implemented by adjusting the speed of the induction motor, and the power required by the mechanical load was controlled. For inverter control, which is a key aspect in a PV system, a space-vector pulse-width modulation (SV-PWM) method was employed. Thus, advantages such as low total harmonic distortion (THD), a well-defined output harmonic spectrum, and better DC-link voltage utilization were achieved.

The paper is organized as follows. Section 2 explains the ANN-based MPPT algorithm. In Section 3, the GA used for training data optimization in the MPPT controller is discussed. Section 4 presents an experimental description and the software implementation of the system. The constant variable frequency volts-per-Hertz (V/f) control and space-vector PWM methods are also briefly explained in Section 4. In Section 5, the simulation and experimental results obtained from the proposed PV system are given, and the conclusions are addressed in Section 6.

2. ANN-based MPPT algorithm

The objective of MPPT controllers is to draw maximum power from PV modules for changing solar irradiance (G) and temperature (T) conditions. With that aim, PV modules are matched to the load and maximum power generation is ensured. In our research, PV module voltage was used as the control parameter and a MPPT controller was implemented based on the voltage. The primary concern was to obtain a reference voltage value (V_{MPP}) at which the PV modules operate at the MPP. In this research, an ANN was used to determine the reference voltage in real time, dependent upon G and T. The dataset used to train the ANN was obtained using experimental measurements, and a relation between the inputs (G and T) and output (V_{MPP}) was established. The developed ANN configuration, shown in Figure 1, is a multilayer-perceptron structure including an input

layer, a hidden layer with 5 hidden nodes obtained based on a trial-and-error method, and an output layer.

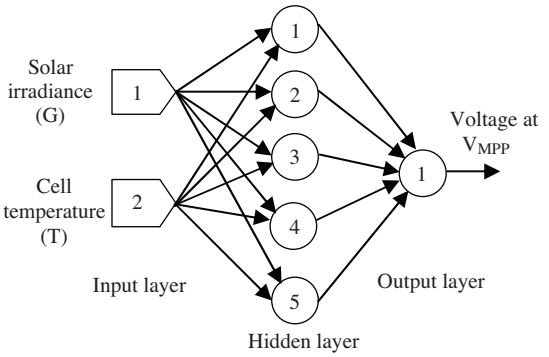

Figure 1. The ANN configuration used to determine the reference voltage value at the MPP.

In order to ensure operation of the MPPT controller in a wide range of operating conditions, the training data must cover a large range. For that purpose, the measurements made to obtain the training dataset covered the range of 91-1105 W/m^2 for irradiance and 11-72.2 °C for cell temperature. A total of 500 measurements were made; 350 of them were used for training, 100 of them were used for cross-validation, and 50 of them were used for testing. The transfer functions of the hidden and output layers were chosen to be tangent hyperbolics. The iteration number was 100 and the error target was 1.10^{-10}.

3. Using GA for training data optimization in MPPT controller

The GA can be used to optimize the input dataset of the ANN to obtain a smaller and more effective input dataset. This method is particularly important if noisy and unimportant data, which reduce the generalization ability and effectiveness of the ANN, are present. The GA can be used to keep the most decisive data and remove insignificant data, and, when using the new dataset, a smaller error value may result at the end of training [6].

In GA optimization of the input dataset, each individual in the population represents the feature subset, which must be solved for the optimization problem. Individuals in the GA are usually represented by n-bit binary vectors. Thus, the search space corresponds to an n-sized Boolean space. In each generation, the evaluation of an individual, i.e. input data, requires the training of the ANN and use of the result in an objective function.

The flowchart used for the GA-based input dataset optimization used in the ANN is shown in Figure 2 [6,11]. At first, the GA creates an initial population, trains the ANN for each chromosome, and evaluates that population. The population then grows with a large number of generations to search for the best input parameters. The generalization performance of the ANN trained with the current dataset is transferred to the GA as a fitness function. The GA continues to operate until a predefined number of generations are complete to generate the population with new numbers. The evaluation is done for each individual in the population. Thus, GA optimization provides an adaptive approach to choosing the most useful and important members of the input dataset [12].

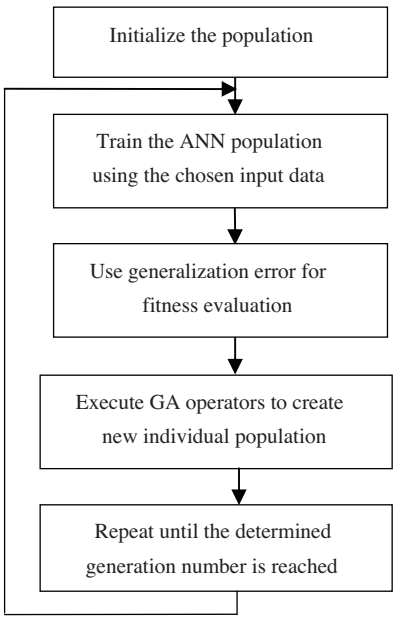

Figure 2. The flowchart for input dataset optimization in ANN.

GAs use fitness-proportionate selection to create individuals for the next generation. Genetic operators are performed on the selected individuals to generate successive generations, and the algorithm explores the space of candidate solutions. Applications of fitness-dependent selection and crossover and mutation genetic operators are repeated until a satisfactory solution is obtained [12]. In practice, the performance of the GA is determined by the genetic representation and the choosing of the operator, fitness-dependent selection, population size, and so on.

The implemented neural network was trained using the Levenberg-Marquardt (LM) algorithm. The Table presents the GA parameters used in GA optimization.

Table. GA parameters used in input data set optimization.

Mutation operator, P_m	0.02
Crossover operator, P_c	0.9
Population size	20
Maximum number of generations	250
Selection type	Roulette
Crossover	Single point

The input dataset optimization algorithm was implemented in a MATLAB environment. The best values of the objective functions over GA generations are shown in Figure 3. As a result of the GA optimization, a new dataset consisting of 187 samples was obtained.

By means of GA optimization in the ANN, better results were obtained than those without using GA optimization. When the ANN was trained without GA optimization, the obtained values for training and cross-validation errors were 0.2137 and 0.2802, respectively. For the ANN trained with the new GA-optimized dataset, the training and cross-validation errors were 0.1806 and 0.2381, respectively. For both of the training algorithms, the training was ended with the early termination method. By this method, when the cross-validation error started to increase, the training was terminated to prevent the ANN from overtraining.

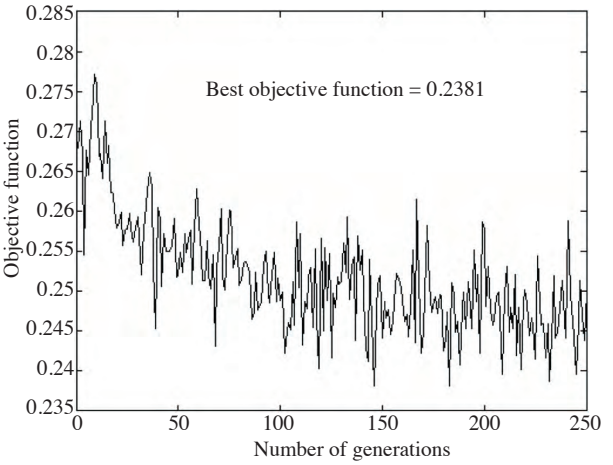

Figure 3. Best values of objective functions over GA generations.

To demonstrate the accuracy of the results obtained from the neural network, random test data with 50 samples, which were not included in the training data, were used. The relative error values, which are the difference between the real values and the ANN output values, are shown for the ANN without GA optimization and for the ANN with GA optimization in Figures 4a and 4b, respectively.

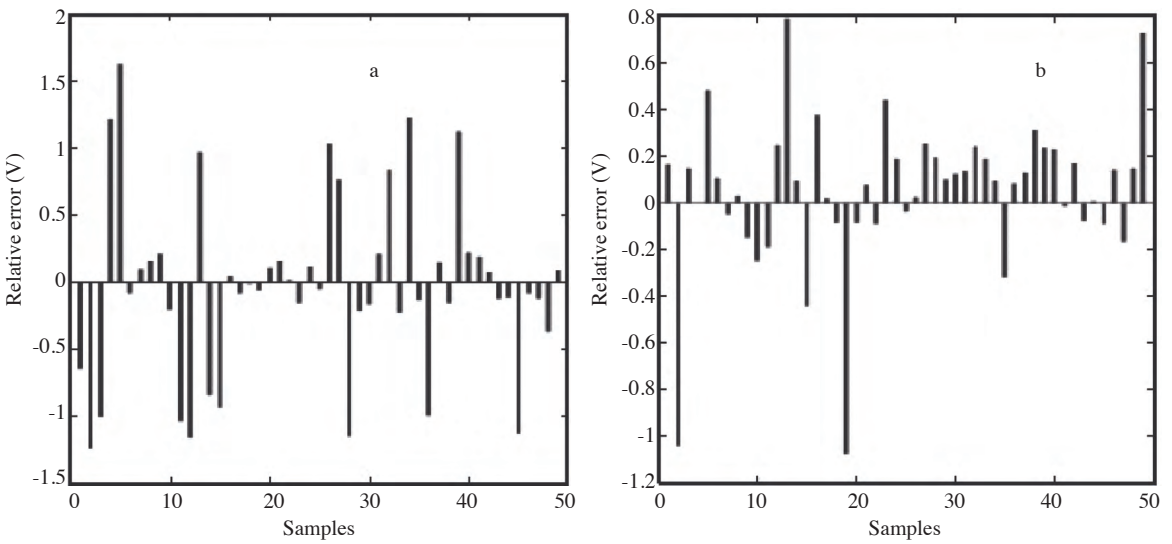

Figure 4. The relative error values for test samples in an ANN trained a) without GA optimization and b) with GA optimization.

Although the training is a very time-consuming and laborious process, this does not pose any difficulties for microcontroller or DSP implementations as the training is implemented once beforehand. The weight and bias values are saved and the ANN structure can be executed offline.

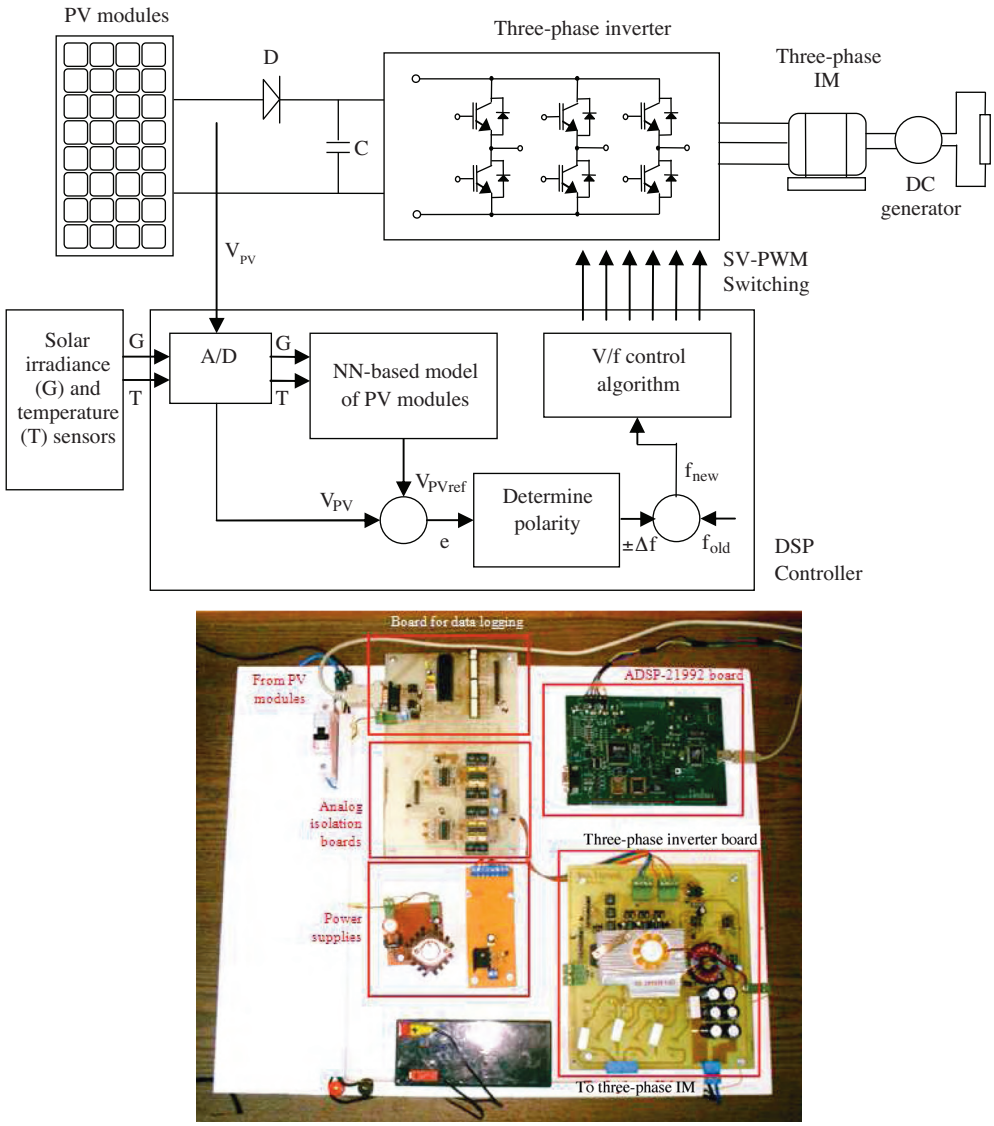

Figure 5. a) Block diagram and b) overview of the proposed PV system.

4. Experimental description and software implementation of the system

The basic configuration of the proposed stand-alone PV system with an ANN-based MPPT controller is shown in Figure 5a. The system was experimentally implemented in the laboratory and an overview of the experimental setup is shown in Figure 5b. The system basically consists of PV modules, a 3-phase inverter, a 3-phase induction motor, a digital signal processor, and other peripherals such as voltage measurement, isolation, and scaling devices. The proposed system was implemented on an ADSP-21992 digital signal processor (DSP) analog device. The DSP unit has a 160-MHz, ADSP-219x DSP core and features an 8-channel, 14-bit, 20-Msps ADC with on-chip voltage reference. It also features a 3-phase PWM generation unit with additional auxiliary PWM outputs, and 3 general-purpose timers of 32 bits.

The system prototype realized in the laboratory consists of 2 series-connected photovoltaic modules, each having a peak power of 60 W [13]. For solar radiation and temperature measurements, a silicon irradiance sensor is used. The sensor has active temperature compensation; its irradiance measurement error with temperature compensation is $\pm 6\%$ and the temperature measurement accuracy at 25 °C is ± 1.5 °C.

The experimental prototype circuit includes an intelligent power module (IPM) [14], which uses insulated-gate bipolar transistors (IGBT). The IPM realizes highly effective over-current and short-circuit protection through the use of advanced current sense IGBT chips that allow continuous monitoring of the power device current. The inverter is rated for 600 V DC and 20 A.

The executed operations implemented in the controller are demonstrated in the flowchart in Figure 6. The controller fundamentally implements a GA-optimized ANN-based MPPT algorithm, a constant V/f control algorithm, and SV-PWM inverter control. Because the output power of the PV modules change nonlinearly with solar irradiance (G) and cell temperature (T), and the proposed system does not include battery back-up, the power induction motor must be operated at varying powers to make full use of the available power. This is achieved by adjusting the motor speed to vary the mechanical power output.

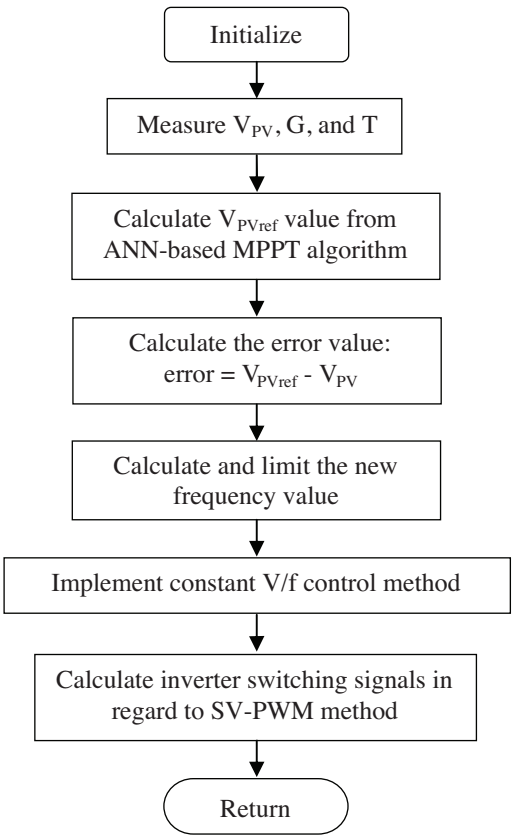

Figure 6. Flowchart of control algorithm.

As shown in Figure 6, the PV modules' output voltage, solar irradiance, and cell temperature values are input into the controller, and the reference voltage value of the PV modules (V_{PVREF}) corresponding to the MPP is calculated by the GA-optimized ANN structure. When the output voltage of the PV modules is adjusted to these values, the system is assumed to operate at the MPP. The error value, which is the difference between reference and measurement values, is obtained and the polarity of the step change of frequency (Δf)

is calculated. The new frequency value is employed in the V/f control algorithm to determine the modulation index (M), and SV-PWM switching signals are synthesized accordingly. Thus, the extracted power from the PV modules is adjusted to its optimum value.

The main control loop, which includes the calculation of the ANN-based MPP of the PV modules, polarity determination of step size, and a constant V/f control algorithm, occurs at a rate of 150 Hz. The calculations required to synthesize the SV-PWM output signal are implemented in an interrupt service routine (ISR) evoked with a frequency of 9 kHz. The switching frequency is also 9 kHz, and ADC sampling is realized every 15 PWM cycles.

In the implemented system, battery back-up is eliminated as the proposed system is mostly suitable for water-pumping applications, which use a water tank for storage, or fan applications, which show a complementary nature for the source and demand sides. The DC-DC converter requirement is also eliminated by implementing a MPPT algorithm in the inverter stage. Therefore, the accompanying losses of these factors could be eliminated.

In the following subsections, the theoretical basis of the implemented constant V/f method and the SV-PWM method are briefly described.

4.1. Constant V/f control

In practice, the rate between the amplitude and frequency is determined by the nominal values of the motor given on its nameplate. However, for lower values of frequency and voltage, the voltage decrease cannot be neglected and must be compensated. In our study, in order to compensate the voltage decrease that occurs due to low stator resistance at low frequencies, the phase voltage was increased for a constant value (C). Thus, as given in Eq. (1), a relationship between the inverter voltage and frequency was used.

$$V = C + kf \tag{1}$$

Here, for $f < f_N$, C is assumed as 0.2, and for $f > f_N$, it is assumed as 0. The f_N value was determined as 20 Hz, and thus the increase in voltage amplitude was provided for $0 \leq f < 20$ Hz. The other constant, k, was determined using motor characteristic values.

4.2. Space-vector PWM method

Space-vector modulation is based on the representation of 3-phase voltages as space vectors. If 3 time-varying quantities sum to 0 and are spatially separated by 120°, then these quantities can be expressed as a single space vector that contains a real (α) and an imaginary (β) component by using the forward Clarke transformation shown in Eq. (2).

$$\begin{bmatrix} V_\alpha \\ V_\beta \end{bmatrix} = \sqrt{\frac{2}{3}} \begin{bmatrix} 1 & -\frac{1}{2} & -\frac{1}{2} \\ 0 & \frac{\sqrt{3}}{2} & -\frac{\sqrt{3}}{2} \end{bmatrix} \begin{bmatrix} V_a \\ V_b \\ V_c \end{bmatrix} \tag{2}$$

As shown in Figure 7, the 8 possible states of an inverter are represented as 2 null vectors and 6 active-state vectors forming a hexagon [6]. The SV-PWM method now approximates the rotating reference vector in each switching cycle by switching between the 2 nearest active-state vectors and the null vectors. In order to maintain the effective switching frequency of the power devices at a minimum, the sequence of toggling between these vectors is organized such that only one leg is affected in every step.

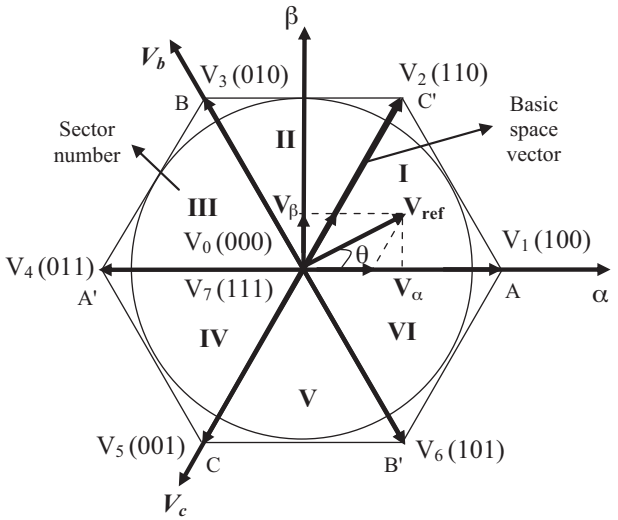

Figure 7. Representation of the inverter states in the stationary reference frame.

Thus, given a space vector of angle θ (in sector 1) and modulation index M, the approximation can be constructed by applying vectors V_1 and V_2 for percentage times T_a and T_b, respectively. The times can be calculated and applied to the appropriate inverter states. The equations for the effective time of the inverter switching states can be given as follows [15].

$$\begin{aligned} T_a &= MT_s \sin(\pi/3 - \theta) \\ T_b &= MT_s \sin\theta \\ T_0 &= T_7 = T_s - T_m \end{aligned} \tag{3}$$

Here, T_a is the time of the switching vector that lags V_{ref}, T_b is the time of the switching vector that leads V_{ref}, T_0 and T_7 are the times of zero-switching vectors, $\mathrm{T}_m = \mathrm{T}_a + \mathrm{T}_b$ is the active modulation time, T_s is the sampling time, and the modulation index M can be given as:

$$M = (\sqrt{3}T_s)/(4V_d), \tag{4}$$

where V_d is the bus voltage of the 3-phase voltage source inverter. The times are distributed to generate symmetrical PWM pulses.

5. Results and discussion

The proposed system was simulated and some experimental results from the laboratory prototype were obtained.

5.1. Simulation results

In order to assess the effectiveness of the proposed PV system with MPPT, simulations were implemented employing a PSIM software tool [16]. In Figure 8, the schematic of the PSIM implementation of the PV system with the proposed GA-optimized ANN-based MPPT algorithm is shown [6].

In Figure 8a, the circuit used to determine the magnitude and direction of reference voltage vector V_{ref} is shown. Using from 3-phase to 2-phase transformations, 3-phase modulation waves are converted into magnitude

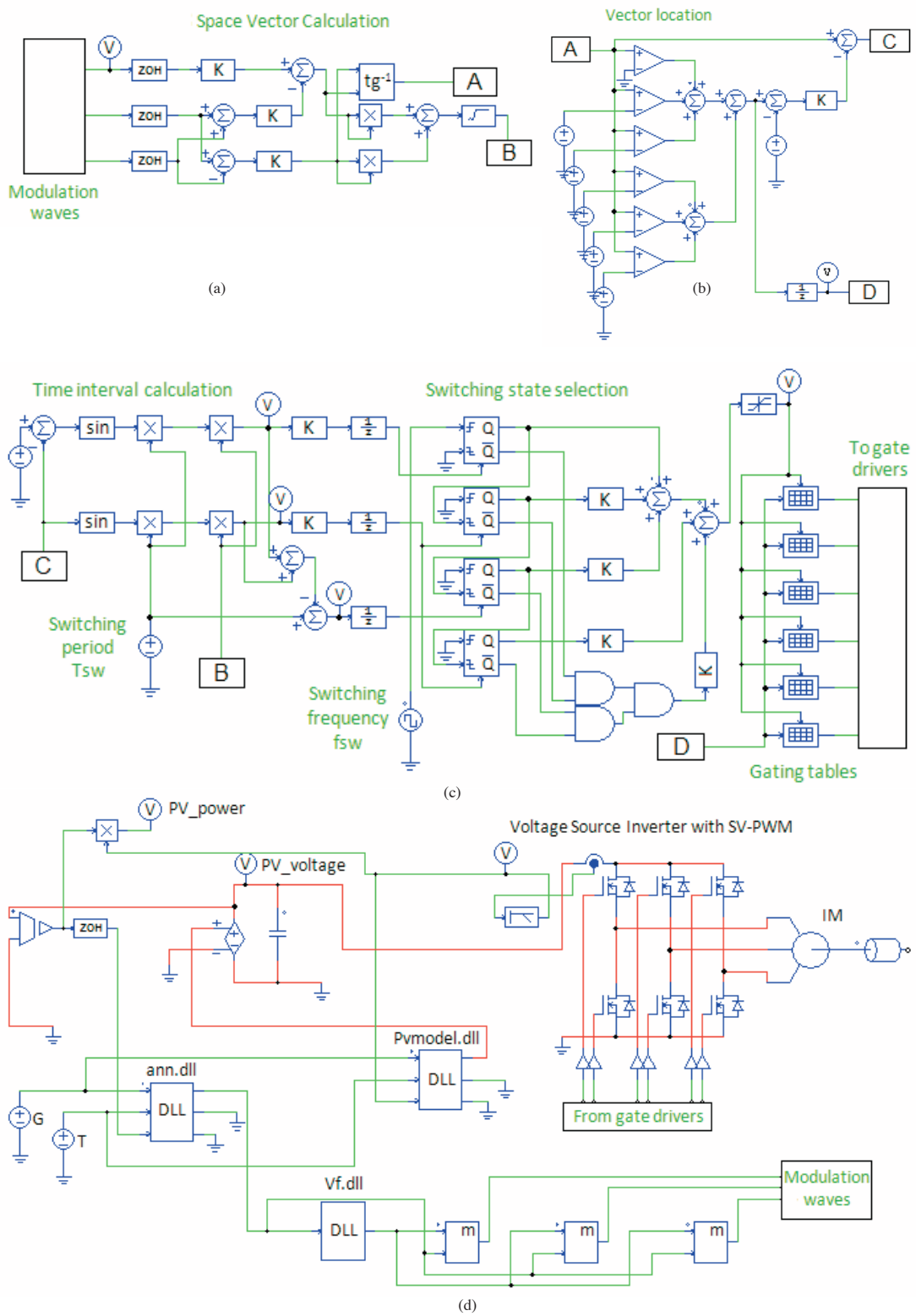

Figure 8. a) Space vector calculation; b) vector location; c) time interval calculation, switching-state selection, and look-up tables for producing signals for gate drivers; d) circuit schematic of the proposed photovoltaic system.

(V_{ref}) and direction (θ). Gain values are given here after processing the 3-phase modulation waves through a 0-order sample-and-hold (ZOH) circuit. A tangential block is used to obtain real and imaginary parts of the expression. It should be noted here that modulation signals are obtained from the ANN-based MPPT algorithm.

The vector location is obtained by the circuit in Figure 8b. Here, the location of the vector is determined by comparators. In Figure 8c, initially, the time interval for which the adjacent vectors must be turned on to get the required reference voltage vector is determined. In the vector location section of the circuit, a controlled monostable multivibrator and AND gates, connected in such a way as to select the various switching states in the space-vector diagram, are used to select a suitable switching state. The switching period and switching frequency are adjusted to the desired values here. Gating tables are 2-dimensional matrix tables consisting of zone numbers as rows and time periods as columns. The conduction periods of predetermined switches are determined by these tables.

The switching signals obtained in regard to the SV-PWM method are used in the 3-phase inverter shown in Figure 8d. Here, the model of the PV modules (PVmodel.dll), proposed ANN-based MPPT algorithm (ann.dll), and V/f control algorithm (Vf.dll) are coded respectively in Visual C++ software and linked to the simulation by dynamic link libraries. Modulation waves were obtained from the proposed ANN-based MPPT algorithm and the SV-PWM switching signals were synthesized in regard to the method explained in Figures 8a-8c.

The simulation curves were obtained for a 3-phase induction motor. Figures 9a and 9b show PV module voltage, current, and power curves obtained in the start-up of the system at a solar irradiance of 915 W/m^2 and a cell temperature of 37 °C for a frequency step change (Δf) of 0.25 and 0.5, respectively.

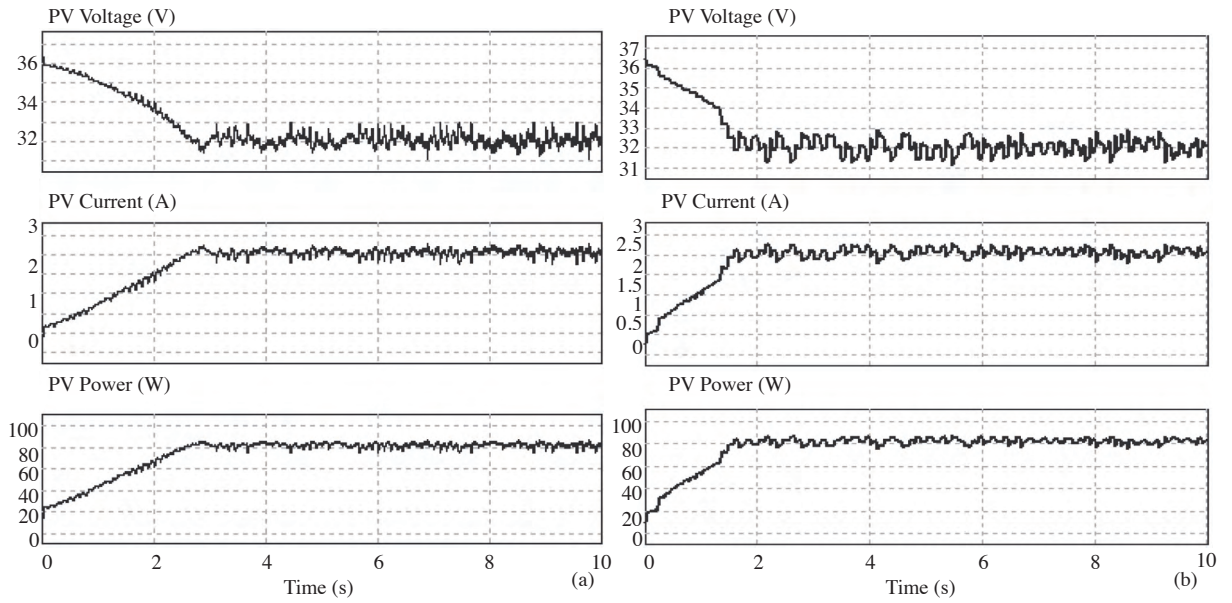

Figure 9. PV module voltage, current, and power curves obtained at the start-up of the system for a) $\Delta f = 0.25$ and b) $\Delta f = 0.5$.

5.2. Experimental results

A laboratory prototype was constructed to study the application of the ANN-based MPPT algorithm on a stand-alone PV system with induction motor drive. To evaluate the effectiveness of the proposed algorithm, the

ANN-based MPPT algorithm with fixed step sizes (chosen as 0.25 and 0.5, respectively) was also programmed in a digital signal processor and both algorithms were tested. The experimental results were obtained in the

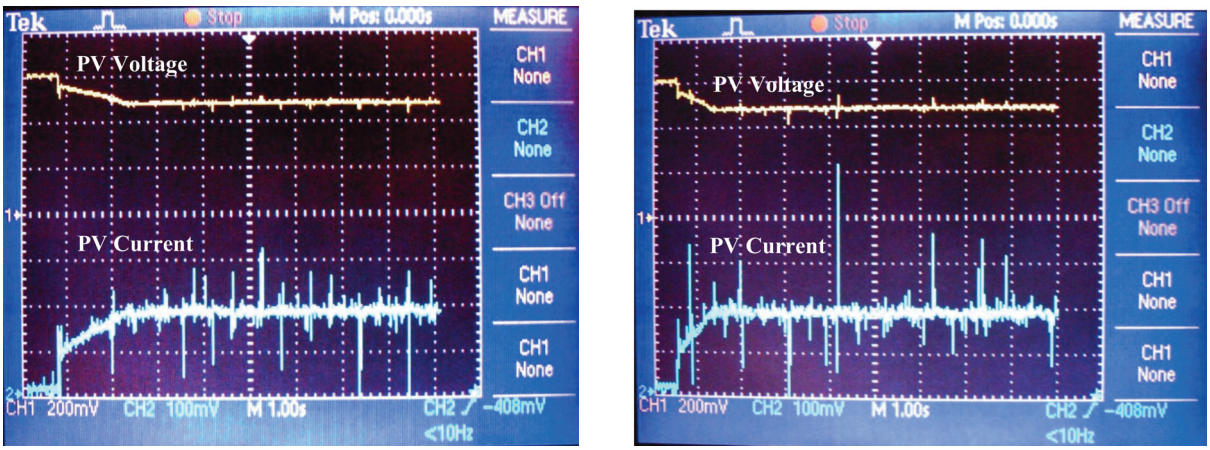

Figure 10. PV module voltage and current waveforms for the step change values of a) $\Delta f = 0.25$ and b) $\Delta f = 0.5$ (volt/div: CH1 13.3 V, CH2 1.5 A; time/div: 1 s).

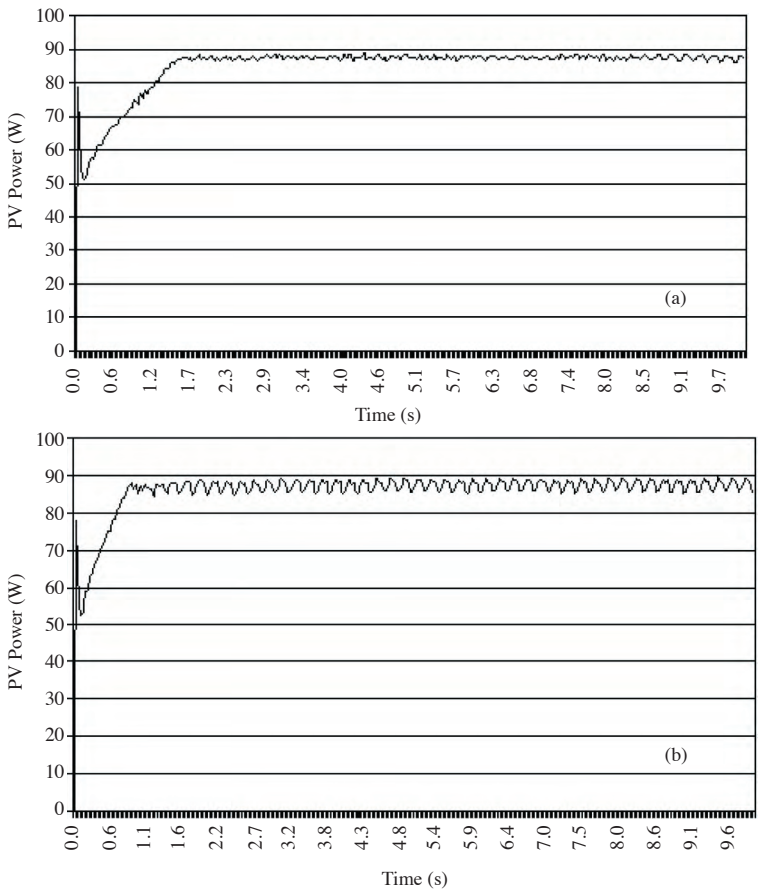

Figure 11. PV module power curves for the step change values of a) $\Delta f = 0.25$ and b) $\Delta f = 0.5$.

start-up of the system. In Figures 10a and 10b, PV module voltage and current waveforms obtained with the proposed algorithm with fixed step sizes of 0.25 and 0.5, respectively, are shown. The results were obtained for a solar irradiance value of 915 W/m^2 and a cell temperature of 37 °C. The power curves calculated from the recorded values of PV voltage and current are respectively shown in Figures 11a and 11b. As shown here, choosing a small value for the step size reduces the speed of reaching the MPP. However, the oscillations around the peak power point are reduced. For a higher step-size value, although the peak power point is reached faster, the oscillations increase.

6. Conclusions

The proposed GA-optimized ANN-based MPPT algorithm was implemented on a stand-alone PV system with a direct-coupled induction motor drive. By means of the proposed algorithm, the requirement of any prior knowledge and the laborious process of obtaining module parameters were eliminated and more accurate results than those of the algorithm without using the GA optimization were obtained.

Compared with the conventional P&O MPPT method, the proposed ANN-based method improved the transitional state and reduced the oscillations in steady state, as the maximum power point was obtained beforehand by the ANN model. Implementing the control algorithm with a variable step size by using a control method such as a proportional-integral controller or a fuzzy logic controller can further improve the tracking ability and efficiency of the PV system.

By implementing the MPPT algorithm in the inverter stage, the requirement of a DC/DC converter was eliminated and, thus, switching elements, their losses, and the requirement of using a bulky inductor in the DC/DC converter stage were eliminated.

Employing the SV-PWM method for the inverter provided advantages such as a wide linear modulation range, less switching loss because of the prevention of unnecessary switching, better utilization of DC-link voltage, and lower base-band harmonics than in regular PWM.

Acknowledgments

The authors would like to acknowledge the Selçuk University Scientific Research Projects (BAP) Coordinating Office for the financial support given under Grant No. 2002/226. The authors would also like to acknowledge POWERSYS for providing the PSIM software (student version).

References

[1] V. Salas, E. Olias, A. Barrado, A. Lazaro, "Review of the maximum power point tracking algorithms for standalone photovoltaic systems", Solar Energy Materials & Solar Cells, Vol. 90, pp. 1555-1578, 2006.

[2] C.R. Sullivan, M.J. Powers, "A high-efficiency maximum power point tracker for photovoltaic arrays in a solar-powered race vehicle", Proceedings of the IEEE Power Electronics Specialists Conference, pp. 574-580, 1993.

[3] J.A. Gow, C.D. Manning, "Controller arrangement for boost converter systems sourced from solar photovoltaic arrays or other maximum power sources", IEE Proceedings - Electric Power Applications, Vol. 147, pp. 15-20, 2000.

[4] K.H. Hussein, I. Muta, T. Hoshino, M. Osakada, "Maximum photovoltaic power tracking: an algorithm for rapidly changing atmosphere conditions", Proceedings of the IEE - Generation, Transmission, and Distribution, Vol. 142, pp. 59-64, 1995.

[5] M. Veerachary, T. Senjyu, K. Uezato, "Neural-network-based maximum-power-point tracking of coupled-inductor interleaved-boost converter supplied PV system using fuzzy controller", IEEE Transactions on Industrial Electronics, Vol. 50, pp. 749-758, 2003.

[6] A.A. Kulaksız, "ANN-based control of a PV system with maximum power point tracker and SVM inverter", Ph.D. Dissertation, Selçuk University Graduate School of Natural and Applied Sciences, Department of Electrical and Electronics Engineering, Konya, Turkey, 2007.

[7] A.B.G. Bahgat, N.H. Helwa, G.E. Ahmad, E.T. El Shenawy, "Maximum power point traking controller for PV systems using neural networks", Renewable Energy, Vol. 30, pp. 1257-1268, 2005.

[8] R. Akkaya, A.A. Kulaksız, O. Aydoğdu, "DSP implementation of a PV system with GA-MLP-NN based MPPT controller supplying BLDC motor drive", Energy Conversion and Management, Vol. 48, pp. 210-218, 2007.

[9] F.Z. Brill, D.E. Brown, W.N. Martin, "Fast genetic selection of features for neural network classifiers", IEEE Transactions on Neural Networks, Vol. 3, pp. 324-328, 1992.

[10] Z. Guo, R.E. Uhrig, "Using genetic algorithms to select inputs for neural networks", Proceedings of the International Workshop on Combinations of Genetic Algorithms and Neural Networks, pp. 223-234, 1992.

[11] A.A. Kulaksız, R. Akkaya, "Training data optimization for ANNs using genetic algorithms to enhance MPPT efficiency of a stand-alone PV system", International Symposium on Innovations in Intelligent Systems and Applications, pp. 523-527, 2010.

[12] J. Yang, V. Honavar, "Feature subset selection using a genetic algorithm", IEEE Intelligent Systems, Vol. 13, pp. 44-49, 1998.

[13] Kyocera Solar, KC60 High Efficiency Multicrystal Photovoltaic Module, available at http://www.kyocerasolar.com/assets/001/5168.pdf.

[14] Mitsubishi Electric, Mitsubishi Intelligent Power Modules PM20CSJ060 Flat-Base Type Insulated Package Datasheet, available at http://pdf1.alldatasheet.com/datasheet-pdf/view/2012/MITSUBISHI/PM20CSJ060.html.

[15] J.O.P. Pinto, B.K. Bose, L.E.B. de Silva, M.P. Kazmierkowski, "A neural-network-based space-vector PWM controller for voltage-fed inverter induction motor drive", IEEE Transactions on Industry Applications, Vol. 36, pp. 1628-1636, 2000.

[16] POWERSYS, PSIM User Manual, available at http://www.psim-europe.com/learningcenter_usermanuals.php.